# Muscle Function and Coordination of Amputee Stair Ascent

**Nicole G. Harper**
Department of Mechanical Engineering,
The University of Texas at Austin,
204 E. Dean Keeton Street, Stop C2200,
Austin, TX 78712
e-mail: Nicole.harper@utexas.edu

**Jason M. Wilken**
Extremity Trauma and Amputation
Center of Excellence,
Center for the Intrepid,
Brooke Army Medical Center,
Ft. Sam, Houston, TX 78234;
Department of Physical Therapy
and Rehabilitation Science,
The University of Iowa,
1-252 Medical Education Building,
Iowa City, IA 52240
e-mail: jason-wilken@uiowa.edu

**Richard R. Neptune**[1]
Department of Mechanical Engineering,
The University of Texas at Austin,
204 E. Dean Keeton Street, Stop C2200,
Austin, TX 78712
e-mail: rneptune@mail.utexas.edu

*Ascending stairs is challenging following transtibial amputation due to the loss of the ankle muscles, which are critical to human movement. Efforts to improve stair ascent following amputation are hindered by the limited understanding of how the prosthesis and remaining muscles contribute to stair ascent. This study developed a three-dimensional (3D) muscle-actuated forward dynamics simulation of amputee stair ascent to identify the contributions of individual muscles and the passive prosthesis to the biomechanical subtasks of stair ascent. The prosthesis was found to provide vertical propulsion throughout stair ascent, similar to nonamputee plantarflexors. However, the timing differed considerably. The prosthesis also contributed to braking, similar to the nonamputee soleus, but to a greater extent. However, the prosthesis was unable to replicate the functions of nonamputee gastrocnemius, which contributes to forward propulsion during the second half of stance and leg swing initiation. To compensate, the hamstrings and vasti of the residual leg increased their contributions to forward propulsion during the first and second halves of stance, respectively. The prosthesis also contributed to medial control, consistent with the nonamputee soleus but not gastrocnemius. Therefore, prosthesis designs that provide additional vertical propulsion as well as forward propulsion, lateral control, and leg swing initiation at appropriate points in the gait cycle could improve amputee stair ascent. However, because nonamputee soleus and gastrocnemius contribute oppositely to many subtasks, it may be necessary to couple the prosthesis, which functions most similarly to soleus, with targeted rehabilitation programs focused on muscle groups that can compensate for gastrocnemius.* [DOI: 10.1115/1.4040772]

## 1 Introduction

Individuals with unilateral transtibial amputations often utilize compensatory mechanisms to restore mobility. The functional loss of the ankle plantarflexors, which are critical contributors to body support, forward propulsion, leg swing, and mediolateral balance [1–4], must be compensated for by either the prosthesis or the remaining muscles of the residual and intact legs. In amputee level walking, this loss and the subsequent compensations often result in increased energy cost [5,6], altered and asymmetric kinematics and kinetics (for review, see Ref. [7]) and diminished balance control [8,9], which suggests that current prostheses are unable to fully compensate for the loss of the plantarflexors.

Stair ascent is a more challenging movement task than level walking because of the additional need to propel the center-of-mass (COM) vertically [10, e.g., 11]. This increased need to elevate the COM is accomplished largely by extending the leg during stance after weight acceptance (Fig. 1). In nonamputees, extension of the leg during stair ascent is accomplished by contributions from the knee extensors [10–13] and ankle plantarflexors [11–13]. However, the loss of the plantarflexors requires amputees to develop compensatory mechanisms which often result in increased lower-limb muscle activity [14,15] and significant asymmetries between the residual and intact legs [14–17] during stair ascent. In the residual leg, amputees often utilize a hip strategy to ascend stairs [16,17], while in the intact leg, they often use ankle [16–18] and knee and hip [15–17] compensations.

Several studies have sought to minimize these compensations and reduce limb asymmetries by assessing the effects of a variety of prosthesis designs on amputee stair ascent [16,19–21]. However, while these studies have noted normalization of some kinematic and kinetic parameters, interlimb asymmetries often still persist [16,21]. One challenge associated with improving prosthesis designs is our limited understanding of how the prosthesis and remaining muscles interact to perform the subtasks of stair ascent.

One approach to determining the underlying contributions from individual muscles and the prosthesis is through muscle-actuated forward dynamics simulations, which have been used to investigate amputee walking [22,23]. These studies found that the prosthesis was able to replicate the functions of soleus by providing a similar amount of body support, but was unable to generate all of the forward propulsion typically provided by the plantarflexors or leg swing initiation typically provided by the gastrocnemius [22,23]. In addition, these studies found significant muscle compensations in the residual and intact legs compared to nonamputee walking. Forward dynamics simulations, as well as other techniques for quantifying muscle function, have also been used to investigate nonamputee stair ascent and have found that the plantarflexors are key contributors to the biomechanical subtasks of stair ascent [24,25]. Thus, compared to nonamputees, amputees likely require altered contributions from the remaining muscles in both the residual and intact legs to overcome the loss of the plantarflexors and limitations in the prosthesis design in order to ascend stairs.

The purpose of this study was to develop a three-dimensional (3D) muscle-actuated forward dynamics simulation of stair ascent following unilateral transtibial amputation to identify the contributions of individual muscles and passive prosthesis to the biomechanical subtasks of stair ascent including vertical propulsion, anteroposterior (AP) propulsion, mediolateral control (i.e., movement of the COM in the mediolateral direction) and leg swing. Identifying these contributions will help clarify the compensatory mechanisms used following transtibial amputation and guide the design and development of improved prostheses and

[1]Corresponding author.
Manuscript received November 23, 2017; final manuscript received June 22, 2018; published online September 25, 2018. Assoc. Editor: Tammy L. Haut Donahue.

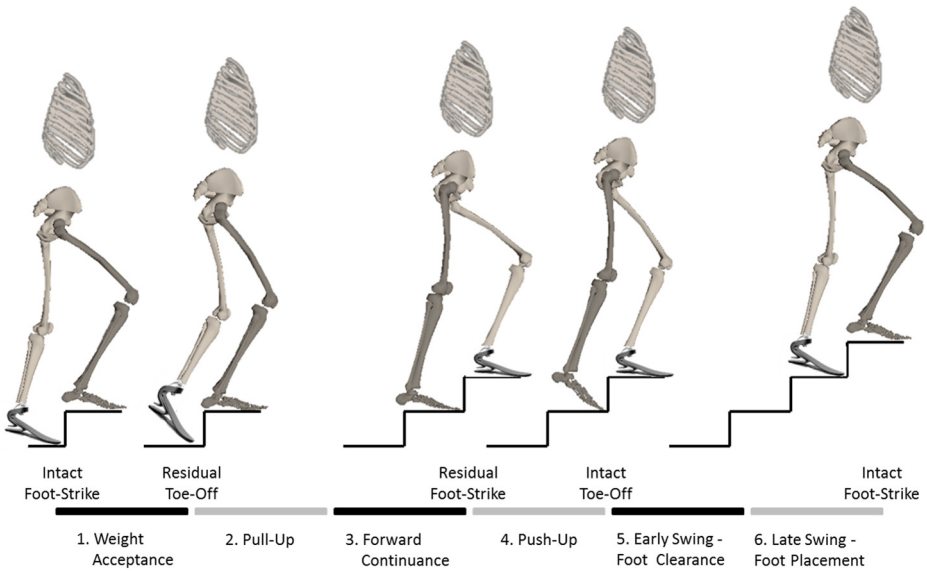


**Fig. 1 The six regions of the intact leg (dark shaded leg) gait cycle: (1) weight acceptance (intact foot-strike to residual toe-off), (2) pull-up and (3) forward continuance (residual toe-off to residual foot-strike divided into two equal regions), (4) push-up (residual foot-strike to intact toe-off), (5) early swing—foot clearance, and (6) late swing—foot placement (intact toe-off to intact foot-strike divided into two equal regions)**

targeted rehabilitation programs aimed at enhancing an amputee's ability to ascend stairs.

## 2 Methods

A three-dimensional muscle-actuated forward dynamics simulation of amputee stair ascent was developed by modeling the musculoskeletal system, passive prosthesis, foot-ground contact, and muscle force generation. Dynamic optimization was then used to identify the muscle excitation patterns that produce a representative simulation of amputee stair ascent. The optimized muscle excitation patterns minimized the differences between the simulated and group-averaged experimental joint kinematics and ground reaction forces (GRFs) for ten subjects with unilateral transtibial amputations. The contributions of individual muscles and the prosthesis to the biomechanical subtasks of stair ascent were then identified using GRF decomposition and segment power analyses. These steps are described below in greater detail.

**2.1 Musculoskeletal Model.** A previously developed three-dimensional bipedal musculoskeletal model [24] was modified to represent a unilateral transtibial amputee. The model was developed using SIMM/Dynamics Pipeline (MusculoGraphics, Inc., Santa Rosa, CA) with previously defined musculoskeletal geometry [26] and consisted of 14 rigid body segments representing the head-arms-trunk (HAT), pelvis and bilaterally the thigh, shank, patella, talus, calcaneus, and toes. The segments were articulated with a total of 23 degrees-of-freedom (DOF), including a 6DOF (three translations, three rotations) joint between the pelvis and ground, 3DOF spherical joints between the trunk and pelvis and at each hip, and 1DOF revolute joints at each knee, ankle, subtalar, and metatarsal joint. To model the altered mass and inertia of the prosthesis, the mass of the residual shank was reduced by 50% compared to the intact shank and the residual shank COM was shifted proximally to be 25% of the knee-to-ankle distance below the knee [23]. In addition, to represent a unilateral transtibial amputee, the muscles spanning the ankle joint were removed from the residual leg (Table 1). The model was driven by the remaining 69 muscles (38 on the intact leg and 31 on the residual leg) and a passive energy storage and return (ESAR) prosthesis.

To model the prosthesis, the average experimental amputee ankle moment data was fit with a second-order torsional spring and damper using the following regression model [23]:

$$\tau = C_0 + C_1\theta + C_2\dot{\theta} + C_3\theta^2 + C_4\theta\dot{\theta} \tag{1}$$

where $\tau$ is the torque applied by the prosthesis, $C_i$ represents the coefficients ($i$ equal to 0–4) determined by fitting the experimental data with the model, $\theta$ is the ankle angle, and $\dot{\theta}$ is the ankle angular velocity. The prosthesis torque determined in Eq. (1) was then applied as a passive torque to the ankle joint. In addition, passive torques representing the forces generated by passive tissues and joint structures were applied at each joint [27]. To model foot-ground contact, 31 viscoelastic elements with Coulomb friction were attached to each foot and evenly distributed across the prosthetic foot as well as the intact calcaneus and toes [28]. The system equations of motion were generated using SD/FAST (PTC, Needham, MA).

Muscle excitations at time $t$ ($e(t)$, Eq. (2)) for the 69 musculotendon actuators were represented using bimodal excitation patterns as

$$e(t) = \sum_{i=1}^{2} \begin{cases} \frac{A_i}{2}\left(1 - \cos\left(\frac{2\pi(t - \text{on set}_i)}{\text{off set}_i - \text{on set}_i}\right)\right) & \text{on set}_i \le t \le \text{off set}_i \\ 0 & t < \text{on set}_i \,||\, t > \text{off set}_i \end{cases} \tag{2}$$

where the onset, offset and amplitude ($A$) of each mode ($i$) were the optimization parameters for each muscle. Muscle activation and deactivation dynamics were modeled using a nonlinear first-order differential equation [29] with previously derived activation and deactivation time constants [30]. Muscle contraction dynamics were governed by hill-type muscle properties [31].

**2.2 Dynamic Optimization.** The simulation was generated over 120% of the gait cycle (from intact foot-strike to the second residual toe-off) using a simulated annealing optimization algorithm [32] that identified the optimal excitation parameters for each muscle (timing and amplitude) that minimized the objective function. The objective function was formulated to (1) achieve

optimal tracking by minimizing the differences between simulated and experimental joint kinematics and GRFs, and (2) eliminate unnecessary muscle co-activation by minimizing total muscle stress. To assess the overall quality of the simulation, the root-mean-square errors between the simulated and experimental kinematics and GRFs were analyzed and the timings of the simulated muscle excitations were compared with EMG timings available in the literature [14,15].

**2.3 Simulation Analyses.** To identify the contributions of individual muscles and prosthesis to the biomechanical subtasks of stair ascent, GRF decomposition and segment power analyses [33,34] were performed. The contributions to vertical propulsion, anteroposterior propulsion and mediolateral control during the first (weight acceptance through pull-up; Fig. 1) and second (forward continuance through push-up; Fig. 1) halves of stance were quantified by contributions to the vertical, AP and mediolateral (ML) GRF, respectively, during each region. The contributions to leg swing were quantified by the power delivered to the leg during swing initiation (push-up; Fig. 1), early swing (early swing—foot clearance; Fig. 1) and late swing (late swing—foot placement; Fig. 1). In addition, throughout stance the mechanical power generated, absorbed and transferred by each muscle and the prosthesis to the trunk (HAT), residual leg and intact leg was determined in the vertical, AP and ML directions. Positive (negative) contributions to the AP and ML GRFs indicated contributions to forward propulsion (braking) and lateral (medial) control, respectively, while positive (negative) power indicates acceleration (deceleration) of the segment in the direction of motion. For analysis, muscles with similar biomechanical function and anatomical classification were combined into 15 muscle groups in the intact leg and 12 muscle groups in the residual leg (Table 1). The contribution of each muscle group was determined by summing the contributions of the individual muscles within each group. The contribution of gravity was also determined since it has been shown to be important in both level walking [35,36] and non-amputee stair ascent [24].

**2.4 Experimental Data.** Ten subjects with traumatic unilateral transtibial amputations (10 male; 29.4±5.7 years; 87.4±13.6 kg; 1.8±0.1 m) and prescribed ESAR prostheses (see Supplemental Table 1, which is available under the "Supplemental Data" tab for this paper on the ASME Digital Collection) participated in this institutionally approved study, which was conducted in the Military Performance Laboratory at the Center for the Intrepid in Fort Sam Houston, TX. All subjects were capable of walking independently for a minimum of 15 minutes, had been independent walkers for a minimum of 5 months and had no comorbidities in the intact leg. Written informed consent was obtained from each subject before they completed the experimental protocol that included ascending a 16-step instrumented staircase (two forceplates, 1200 Hz: AMTI, Inc., Watertown, MA) step-over-step at a fixed cadence of 80 steps per minute. An interlaced staircase design was used (similar to Ref. [37]) so that the first forceplate recorded kinetic data from steps five and seven and the second forceplate recorded kinetic data from steps six and eight. Three-dimensional body segment kinematics were collected using a 26-camera optoelectronic motion capture system (120 Hz, Motion Analysis Corp., Santa Rosa, CA) and a marker set consisting of 57 reflective markers [38]. A digitizing wand was used to identify bony landmarks to align segment coordinate systems with bony anatomy (C-Motion, Inc., Germantown, MD).

Biomechanical data were processed in Visual3D (C-motion, Inc., Germantown, MD). A 13-segment model was scaled to each subject's body mass and height [39] using the anatomical bony landmarks to define the joint centers and joint coordinate systems [40–42]. Marker and GRF data were low-pass filtered using a fourth-order Butterworth filter with cut-off frequencies of 6 Hz and 50 Hz, respectively. Joint kinematics were computed using Euler angles with previously defined pelvis, hip, knee, and ankle Cardan rotation sequences [40,42,43]. For five complete gait cycles for each leg, GRFs were normalized by subject body weight and both GRFs and three-dimensional joint kinematics were time-normalized to 100% of the gait cycle and exported to MATLAB (MathWorks, Inc., Natick, MA), where they were averaged across gait cycles and subjects for each leg.

## 3 Results

The mechanical power generated, absorbed, and transferred by each muscle to the trunk (HAT), residual leg and intact leg in each direction can be found in the Supplemental Results, which are available under the "Supplemental Data" tab for this paper on the ASME Digital Collection. The power distributions for the plantarflexors and prosthesis will be presented here.

**3.1 Simulation Quality.** The simulated kinematics and GRFs produced by the optimal set of muscle excitations emulated the experimental data, with quantities within two standard deviations

**Table 1 Muscles included in the musculoskeletal model and their corresponding analysis groups in both the intact and residual legs. The muscles labeled as "REMOVED" have been removed from the residual leg.**

| | Analysis groups | |
|---|---|---|
| Muscles | Intact leg | Residual leg |
| Iliacus<br>Psoas | IL | IL |
| Adductor Longus<br>Adductor Brevis<br>Pectineus<br>Quadratus Femoris | AL | AL |
| Superior Adductor Magnus<br>Middle Adductor Magnus<br>Inferior Adductor Magnus | AM | AM |
| Sartorius | SAR | SAR |
| Rectus Femoris | RF | RF |
| Vastus Medialis<br>Vastus Lateralis<br>Vastus Intermedius | VAS | VAS |
| Anterior Gluteus Medius<br>Middle Gluteus Medius<br>Anterior Gluteus Minimus<br>Middle Gluteus Minimus | GMEDA | GMEDA |
| Posterior Gluteus Medius<br>Posterior Gluteus Minimus<br>Piriformis<br>Gemellus | GMEDP | GMEDP |
| Tensor Fasciae Latae | TFL | TFL |
| Superior Gluteus Maximus<br>Middle Gluteus Maximus<br>Inferior Gluteus Maximus | GMAX | GMAX |
| Semitendinosus<br>Semimembranosus<br>Gracilis<br>Biceps Femoris Long Head | HAM | HAM |
| Biceps Femoris Short Head | BFSH | BFSH |
| Medial Gastrocnemius<br>Lateral Gastrocnemius | GAS | Removed |
| Soleus<br>Tibialis Posterior<br>Flexor Digitorum Longus | SOL | Removed |
| Tibialis Anterior<br>Extensor Digitorum Longus | TA | Removed |

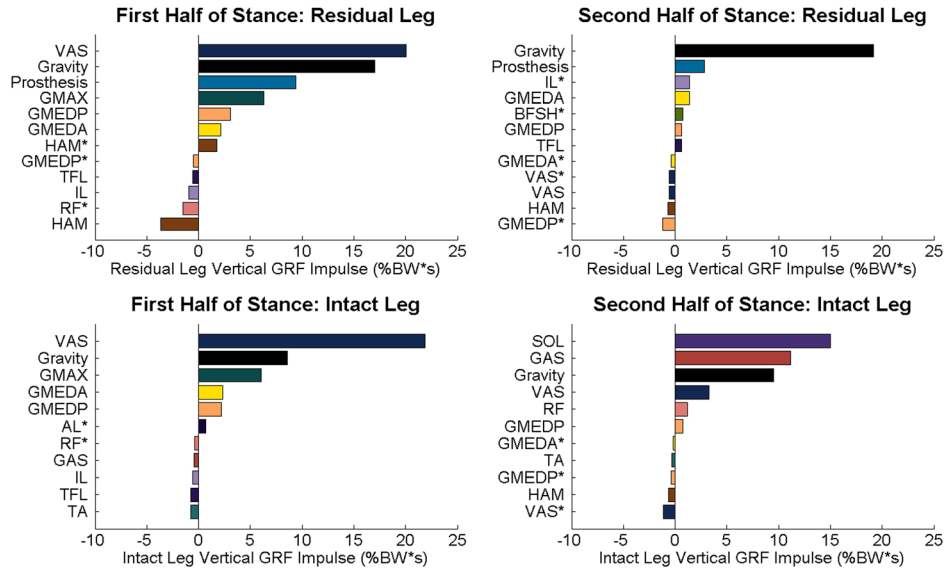


**Fig. 2 Primary positive and negative contributors to vertical propulsion of the body COM (i.e., the vertical GRF impulse) during the two halves of residual and intact leg stance: (1) weight acceptance through pull-up, and (2) forward continuance through push-up. Muscle names without an asterisk (*) are from the leg specified in the plot title while muscle names with an asterisk (*) are from the contralateral leg. For muscle group abbreviations, see Table 1.**

(SDs) for most of the gait cycle. Thus, overall the simulation fell within a normal distribution of the experimental data and was considered consistent with the mechanics of ascending stairs following transtibial amputation. The average root-mean-square error between the simulated and experimental pelvis translations, joint kinematics and GRFs across the gait cycle was 0.037 m (2 SDs = 0.101 m), 9.14 deg (2 SDs = 11.31 deg) and 0.128% body weight (2 SDs = 0.099%BW), respectively. In addition, the timing profiles of the optimized muscle excitations were similar to the EMG data available in the literature (Supplemental Fig. 1, which is available under the "Supplemental Data" tab for this paper on the ASME Digital Collection).

**3.2 Vertical Propulsion.** The primary contributors to vertical propulsion during the first half of stance were similar in both the residual and intact legs with primary contributions from VAS and additional contributions from GMAX, GMEDA and GMEDP (Fig. 2). In the residual leg, the prosthesis also contributed critically to vertical propulsion (Fig. 2) by providing power to the trunk and residual leg (Fig. 3), while HAM opposed vertical propulsion (Fig. 2). In the second half of stance, the primary contributors to vertical propulsion in the intact leg were the plantarflexors (Fig. 2), which generated power to the trunk and intact leg (Fig. 3), while the prosthesis was a primary contributor in the residual leg (Fig. 2). In contrast to the intact plantarflexors, the prosthesis absorbed power from the trunk and residual leg while transferring some power to the intact leg (Fig. 3). At the end of residual leg stance, the pelvis was moving downward; therefore, by absorbing power from the trunk the prosthesis decelerated the pelvis' downward motion and contributed to vertical propulsion. Gravity was also a predominant contributor to the vertical GRF throughout stance, particularly in the residual leg.

**3.3 Anteroposterior Propulsion.** During the first half of stance, the primary contributors to forward propulsion in the intact and residual legs were GMAX and HAM, respectively (Fig. 4).

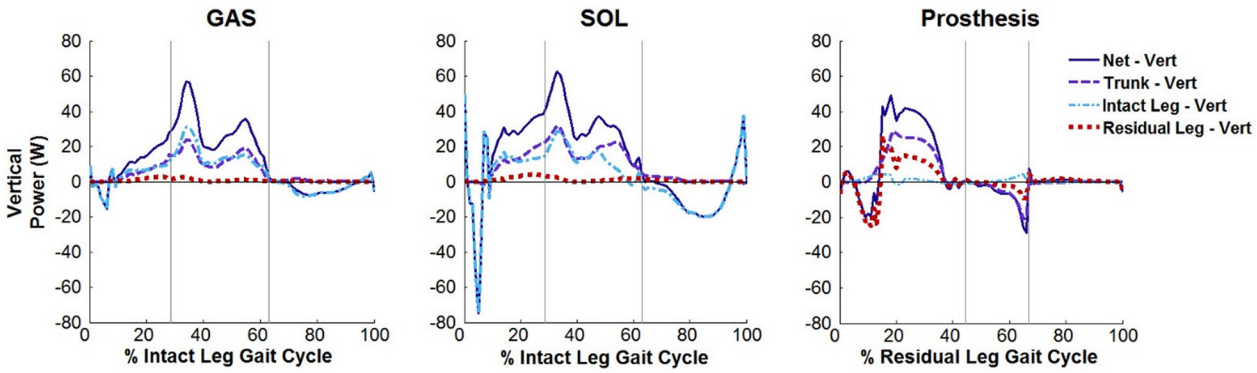


**Fig. 3 Musculotendon mechanical power output from the intact plantarflexors (gastrocnemius: GAS; soleus: SOL) and the prosthesis across the intact and residual leg gait cycles, respectively, and distributed to the trunk, intact leg and residual leg in the vertical direction. Positive (negative) net values indicate power generated (absorbed) by the musculotendon actuator. Positive (negative) values for the leg or trunk indicate that power is being generated to (absorbed from) the leg or trunk. The gray lines divide the gait cycle into three regions: (1) weight acceptance through pull-up, (2) forward continuance through push-up, and (3) swing (foot clearance through foot placement).**

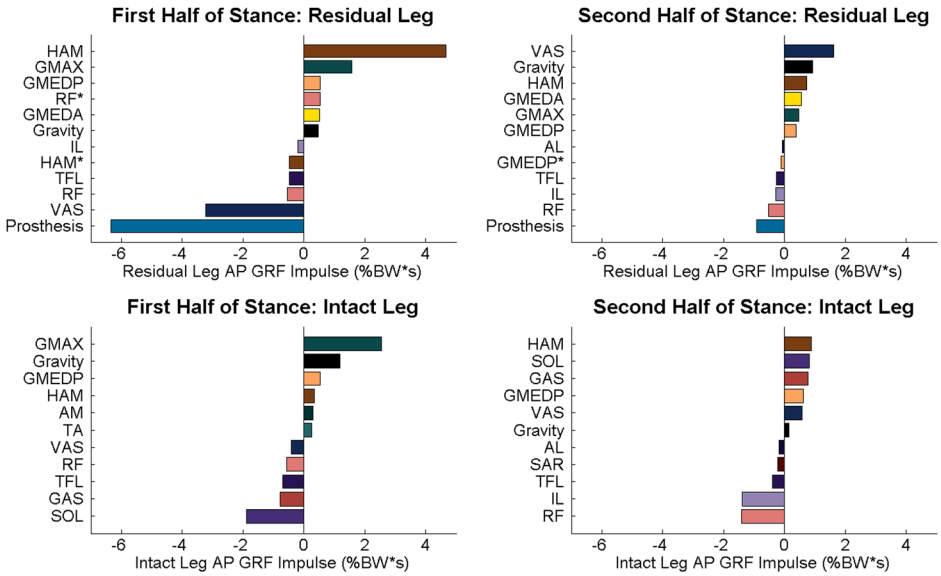


**Fig. 4 Primary positive and negative contributors to AP propulsion of the body COM (i.e., the AP GRF impulse) during the two halves of intact and residual leg stance: (1) weight acceptance through pull-up, and (2) forward continuance through push-up. Positive (negative) GRF impulses indicate contributions to forward propulsion (braking) of the COM. Muscle names without an asterisk (*) are from the leg specified in the plot title while muscle names with an asterisk (*) are from the contralateral leg. For muscle group abbreviations, see Table 1.**

The plantarflexors, primarily SOL, and prosthesis contributed to braking in the intact and residual legs, respectively (Fig. 4), by absorbing AP power from the trunk and/or intact leg (Fig. 5). Gravity contributed to forward propulsion in both legs.

During the second half of stance, the primary contributors to forward propulsion in the intact and residual legs were HAM and VAS, respectively (Fig. 4). In addition, SOL, GAS, GMEDP and VAS contributed to forward propulsion in the intact leg and HAM, GMEDA, GMAX, and GMEDP contributed to forward propulsion in the residual leg (Fig. 4). Gravity also contributed to forward propulsion in both legs, but to a much greater extent in the residual leg. During this region, the prosthesis was the primary contributor to braking in the residual leg (Fig. 4) as it absorbed AP power from the residual leg despite a substantial amount of this power being transferred to the trunk (Fig. 5). In the intact leg, RF and IL were the primary contributors to braking during the second half of stance (Fig. 4).

**3.4 Mediolateral Control.** Throughout stance, GMEDA and GMEDP were the primary contributors to medial control in both the residual and intact legs with additional contributions from RF and TFL in the residual leg during the second half of stance. HAM and VAS were the primary contributors to lateral control in the residual leg while the plantarflexors (SOL and GAS; first half of stance) and hip adductors (AM and AL; second half of stance) were the primary contributors in the intact leg (Fig. 6). Although contributions from the prosthesis were small, the prosthesis contributed to medial control. Gravity contributed to medial control in the intact leg and to lateral (first half of stance) and medial (second half of stance) control in the residual leg. Throughout stance, the plantarflexors contributed to lateral control by transferring ML power from the intact leg to the trunk, while the prosthesis contributed to medial control by providing power directly to the trunk, and to a lesser extent, the legs (Fig. 7).

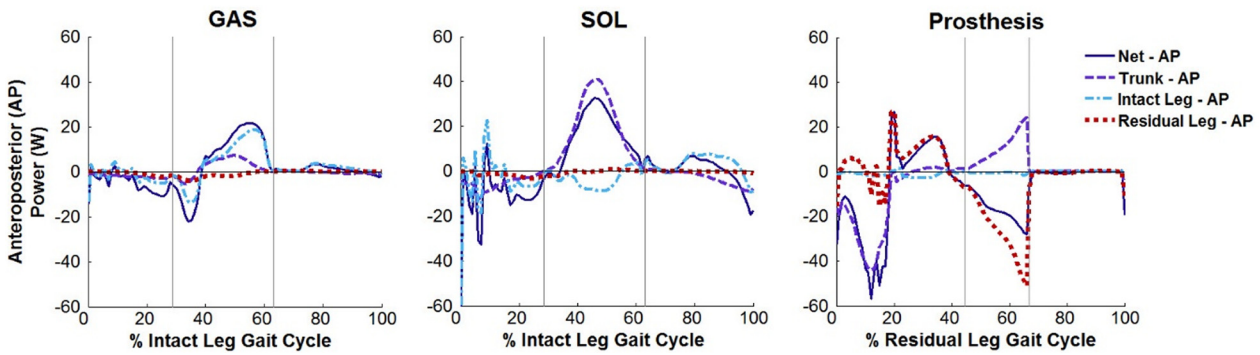


**Fig. 5 Musculotendon mechanical power output from the intact plantarflexors (gastrocnemius: GAS; soleus: SOL) and the prosthesis across the intact and residual leg gait cycles, respectively, and distributed to the trunk, intact leg and residual leg in the AP direction. Positive (negative) net values indicate power generated (absorbed) by the musculotendon actuator. Positive (negative) values for the leg or trunk indicate that power is being generated to (absorbed from) the leg or trunk. The gray lines divide the gait cycle into three regions: (1) weight acceptance through pull-up, (2) forward continuance through push-up, and (3) swing (foot clearance through foot placement).**

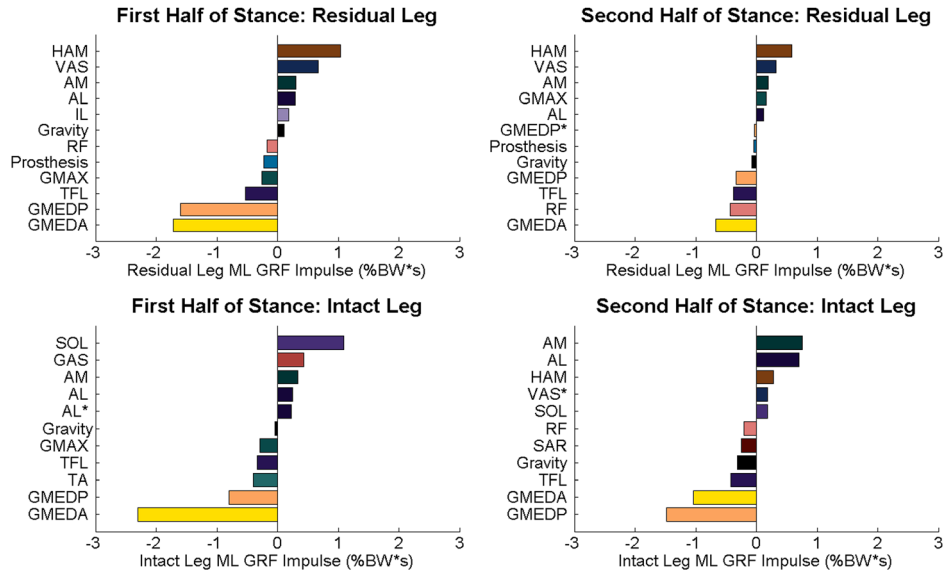


**Fig. 6 Primary positive and negative contributors to ML control of the body COM (i.e., the ML GRF impulse) during the two halves of intact and residual leg stance: (1) weight acceptance through pull-up, and (2) forward continuance through push-up. Positive (negative) GRF impulses indicate contributions to lateral (medial) control of the COM. Muscle names without an asterisk (*) are from the leg specified in the plot title while muscle names with an asterisk (*) are from the contralateral leg. For muscle group abbreviations, see Table 1.**

**3.5 Leg Swing.** During swing initiation of the residual leg, intact HAM, AM, and AL in addition to residual HAM were the primary generators of residual leg power while the prosthesis and residual VAS were the primary absorbers of power from the residual leg, opposing swing initiation (Fig. 8). The prosthesis absorbed power from the residual leg and transferred some of that power to the trunk, similar to the role of intact SOL during this region (Fig. 9). During residual leg swing (early and late), residual IL was the primary generator of power to the residual leg, while gravity and residual VAS (late swing) were the primary absorbers of power from the residual leg.

During swing initiation of the intact leg, intact AL and IL were the primary generators of power to the intact leg with additional power generation from intact GAS and AM and residual GMEDA (Fig. 8). Similarly, during early swing of the intact leg, intact IL was the primary generator of power with additional power generation from intact RF and AL and residual GMEDA. During these regions, gravity was the primary absorber of power from the residual leg, which decelerated its motion. During late swing, residual HAM and intact GMEDP and TA were the primary generators of power to the intact leg while residual RF and intact AL absorbed power from the intact leg in preparation for contact with the ground.

## 4 Discussion

The purpose of this study was to determine how individual muscles and a passive ESAR prosthesis work in synergy during stair ascent following unilateral transtibial amputation to accomplish the biomechanical subtasks of vertical propulsion, anteroposterior propulsion, mediolateral control, and leg swing. The prosthesis was found to be a critical contributor to these subtasks in the residual leg while the plantarflexors were critical contributors in the intact leg. However, distinct between-limb differences were observed because the prosthesis was unable to replicate all of the contributions of the nonamputee plantarflexors [24]. These

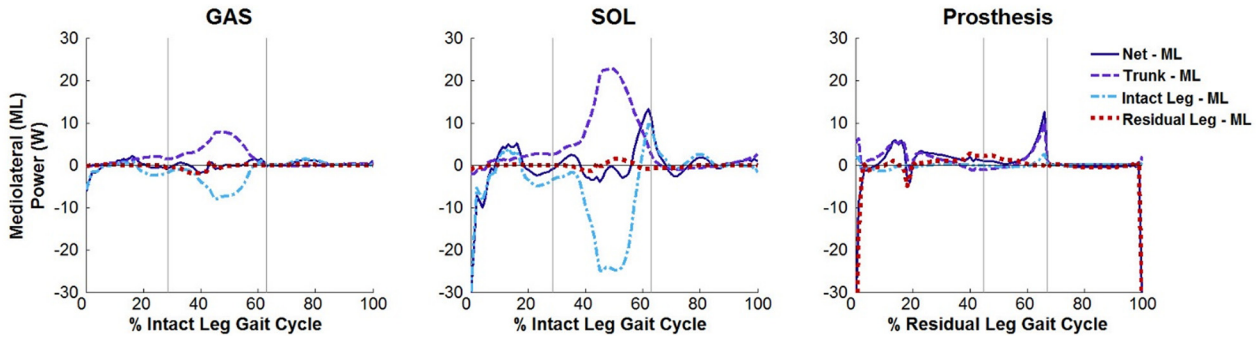


**Fig. 7 Musculotendon mechanical power output from the intact plantarflexors (gastrocnemius: GAS; soleus: SOL) and the prosthesis across the intact and residual leg gait cycles, respectively, and distributed to the trunk, intact leg and residual leg in the ML direction. Positive (negative) net values indicate power generated (absorbed) by the musculotendon actuator. Positive (negative) values for the leg or trunk indicate that power is being generated to (absorbed from) the leg or trunk. The gray lines divide the gait cycle into three regions: (1) weight acceptance through pull-up, (2) forward continuance through push-up, and (3) swing (foot clearance through foot placement).**

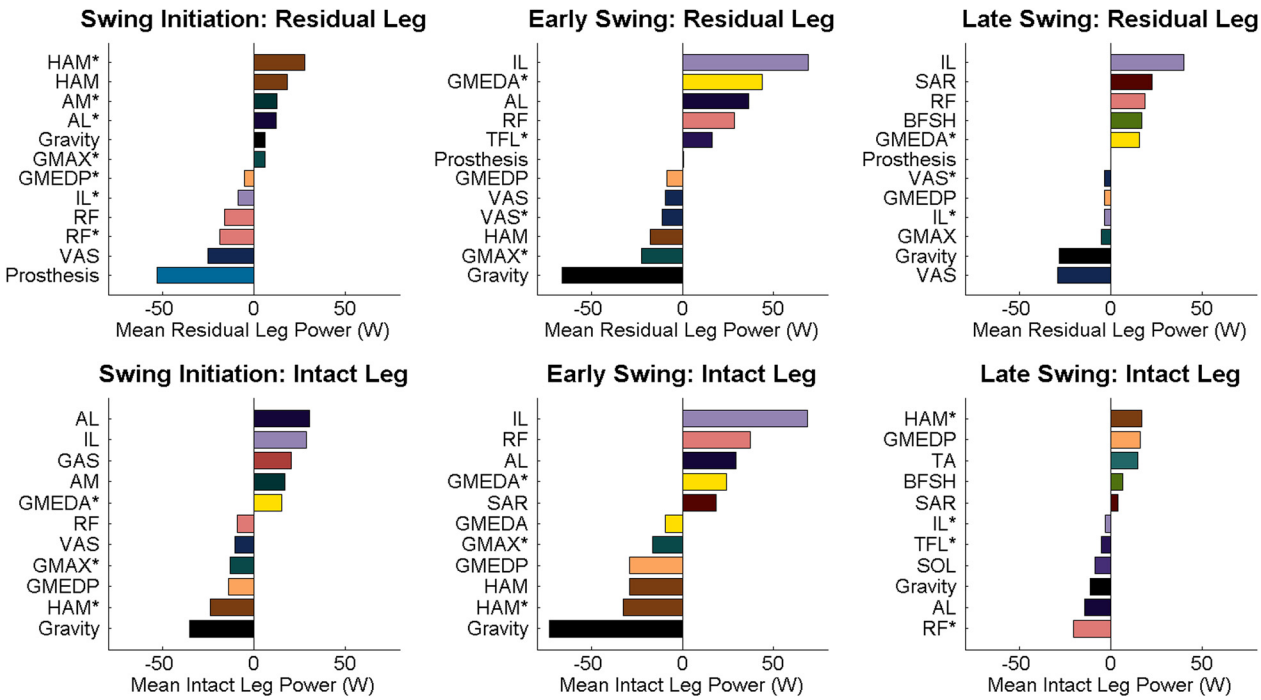


**Fig. 8 Primary contributors to the net mean mechanical power generated (positive) to and absorbed (negative) from the intact and residual legs during: (1) swing initiation (push-up), (2) early swing (foot clearance), and (3) late swing (foot placement). Muscle names without an asterisk (*) are from the leg specified in the plot title while muscle names with an asterisk (*) are from the contralateral leg. For muscle group abbreviations, see Table 1.**

results are consistent with the experimentally observed compensations that arise due to limited prosthesis functionality [14,44].

The primary contributors to vertical propulsion in both legs were largely consistent with the primary contributors in nonamputee stair ascent [24] and amputee level walking [23], with VAS, GMAX, and the prosthesis contributing in the first half of stance and the plantarflexors or prosthesis (to a lesser extent) contributing in the second half. Overall, these results are consistent with previous work that identified a correlation between peak knee and ankle joint power and vertical acceleration during the first and second halves of stance of nonamputee stair ascent, respectively [13]. However, in the present study, the prosthesis provided the majority of its vertical propulsion during the first half of stance, in contrast to the intact and nonamputee plantarflexors [24], which provided vertical propulsion primarily during the second half of stance. In the residual leg, this was compensated for by greater negative contributions from HAM during the first half of stance and by increased contributions from gravity during the second half of stance compared to nonamputee stair ascent [24]. This increased contribution from gravity is consistent with a previous study that found amputees altered their body position to facilitate advancement of the body's center of gravity over the prosthetic ankle during stair ascent [14]. Overall, with some minimal changes in muscle contributions, the prosthesis was able to provide some vertical propulsion in the absence of the plantarflexors, similar to the role of the prosthesis in amputee level walking [22,23]. However, these contributions were provided primarily during the first half of stance and increased contributions from gravity were necessary during the second half of stance.

The primary contributors to anteroposterior propulsion in the intact leg during the first half of stance were similar to the primary contributors in nonamputee stair ascent [24], with GMAX providing the primary contribution to forward propulsion and the intact plantarflexors contributing to braking. Similarly, in the residual

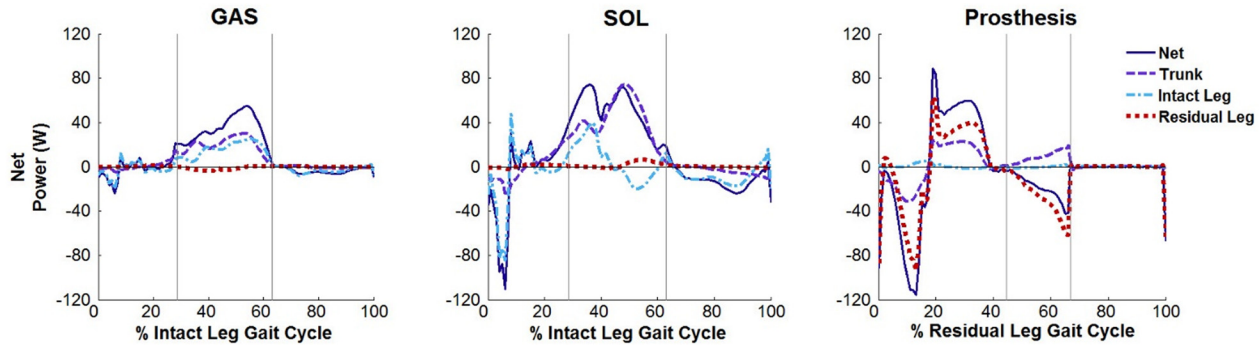


**Fig. 9 Musculotendon mechanical power output from the intact plantarflexors (gastrocnemius: GAS; soleus: SOL) and the prosthesis across the intact and residual leg gait cycles, respectively, and distributed to the trunk, intact leg and residual leg. Positive (negative) net values indicate power generated (absorbed) by the musculotendon actuator. Positive (negative) values for the leg or trunk indicate that power is being generated to (absorbed from) the leg or trunk. The gray lines divide the gait cycle into three regions: (1) weight acceptance through pull-up, (2) forward continuance through push-up, and (3) swing (foot clearance through foot placement).**

leg the prosthesis contributed to braking in this region. However, the prosthesis' contribution to braking was larger than the contribution from the intact or nonamputee [24] plantarflexors and the prosthesis absorbed increased AP power from the trunk, similar to its role in amputee level walking [22]. To compensate for the prosthesis' increased braking, residual HAM increased its contribution to forward propulsion while the intact leg decreased braking contributions from the plantarflexors compared to nonamputee stair ascent [24]. This is consistent with the previous finding that decreased prosthesis mobility during weight acceptance limited an amputee's ability to advance over the foot which necessitated muscle compensations [14,18].

During the second half of stance in the intact leg, HAM and the plantarflexors were important contributors to forward propulsion. While this is consistent with the role of HAM in nonamputee stair ascent, the important contribution of the plantarflexors to forward propulsion is largely contrary to their role in nonamputee stair ascent [24], but consistent with previous studies which found that ankle power generation during the second half of stance was greater in the intact leg compared to the nonamputee leg [17,18,21], and hypothesized that this additional energy generated by the plantarflexors could help propel the trunk onto the residual leg [17]. This finding is also consistent with the role of the plantarflexors in amputee level walking [23]. In the residual leg, the prosthesis contributed to braking, in contrast to its role in amputee level walking [22,23] and to the role of the intact plantarflexors. However, the prosthesis was able to largely replicate the function of nonamputee SOL by providing AP power to the trunk, although it did so by absorbing AP power from the residual leg and was therefore unable to replicate the function of nonamputee GAS [24]. This is consistent with the ability of the prosthesis to replicate the functions of SOL but not GAS during amputee level walking [22,23]. While the role of the prosthesis was similar to nonamputee SOL, the prosthesis generated increased braking during the second half of stance, and to compensate, residual RF decreased its contribution to braking while residual VAS became the primary contributor to forward propulsion. This is in contrast to its contribution to braking in nonamputee stair ascent [24].

Lateral control throughout stance was provided primarily by HAM and VAS in the residual leg and by the plantarflexors (first half of stance) and hip adductors (AM and AL; second half of stance) in the intact leg. The contributions from the hip adductors and HAM to lateral control are consistent with their contributions in amputee level walking [23] and nonamputee stair ascent [24], while VAS's contribution to lateral control is consistent with its contribution in nonamputee stair ascent. Contrary to both nonamputee stair ascent [24] and amputee level walking [23], in amputee stair ascent SOL contributed to lateral control throughout stance and GAS contributed to lateral control during the first half of stance. The prosthesis contributed to medial control (albeit minimally) throughout stance, which is consistent with the role of nonamputee SOL [24] but contrary to the prosthesis' role in amputee level walking [23] and to the role of nonamputee GAS, which contributes to lateral control during the second half of stance.

Throughout stance, medial control was primarily provided by GMEDA and GMEDP, similar to nonamputee stair ascent [24] and amputee level walking [23]. However, their contributions in the intact leg increased to compensate for the increased lateral control provided by the intact plantarflexors. The increased overall contributions to medial and lateral control in amputee stair ascent compared to nonamputee stair ascent are consistent with the increased step width observed in amputees both previously [44] and in the present study, in which increased hip abduction was observed in both legs compared to the nonamputee leg [24]. In addition, the altered muscle contributions to mediolateral control in amputee stair ascent compared to amputee level walking may be indicative of the increased instability of the task [45].

The primary contributors to leg swing in both the intact and residual legs were largely different from nonamputee stair ascent [24] and amputee level walking [23]. However, GAS was an important contributor to swing initiation of the intact leg, similar to its role in nonamputee stair ascent [24] and amputee level walking [23], while SOL decelerated the intact leg in late swing in preparation for contact with the ground, similar to its role in nonamputee stair ascent [24]. During swing initiation, the prosthesis produced a similar power distribution to both the intact and nonamputee SOL [24], transferring power from the ipsilateral leg to the trunk, but was unable to emulate the power distribution produced by the intact or nonamputee GAS, which generated power to both the ipsilateral leg and trunk. This suggests that the prosthesis compromised leg swing and instead transferred power to the trunk, similar to the role of the prosthesis in amputee level walking [22,23]. Although the action of the prosthesis to oppose swing initiation is consistent with the role of SOL in nonamputee stair ascent [24], it contributed to a much greater extent. In response to the prosthesis' increased opposition to swing initiation, the residual leg received increased positive contributions from the intact leg, specifically HAM, AL, and AM. In addition, residual IL and intact GMEDA increased their positive contributions to residual leg swing, consistent with previous work that found increased residual leg hip flexion during swing [21].

Previous experimental studies reporting net joint moments suggest that amputees use a hip-extensor strategy on the residual leg and a knee-extensor strategy on the intact leg during stair ascent [14–17,19,21]. The current study demonstrated that due to the passive nature of the prosthesis, it contributes to vertical propulsion primarily during the first half of stance and is largely unable to emulate the vertical propulsion of nonamputee SOL and GAS during the second half of stance. This inability of the prosthesis to elevate the COM during the push-up phase is thought to result in increased reliance on the intact leg knee extensors. This increase was not, however, observed in our modeling results. There is also no evidence of reliance on residual leg hip extensors for vertical propulsion during the first half of stance. The experimentally observed increase in the hip joint moment may, however, be associated with anteroposterior propulsion rather than vertical propulsion. The large braking effect of the prosthesis during early stance and associated residual knee extensor moment during the first half of stance, which are thought to require a hip-extensor strategy, are evident in Figs. 4 and 5. There is also a large corresponding increase in the contribution of residual HAM during the first half of residual leg stance. Therefore the observed changes in residual leg moments associated with a hip strategy appear to be associated with anteroposterior propulsion rather than vertical propulsion. These results highlight the importance of using modeling and simulation techniques to investigate individual muscle function and identify contributions from muscles that may seem less important at the joint level, but due to dynamic coupling [46,47], actually play a critical role in task execution.

Thus, musculoskeletal modeling and simulation techniques can provide valuable insight into quantities that cannot be measured experimentally. However, one limitation of these simulations is that the results cannot be directly validated by experimental data. In this study, a biomechanically consistent simulation was produced by requiring the simulation to closely replicate experimental data while also minimizing muscle co-contraction. In addition, simulated muscle excitation timings were compared to the experimental timings available in the literature for unilateral transtibial amputees [14,15], and although differences were evident (Supplemental Fig. 1, which is available under the "Supplemental Data" tab for this paper on the ASME Digital Collection), these differences were similar to the variability observed between the experimental studies. However, the availability of experimental timings in the literature was limited. Thus, an additional limitation is that experimental EMG data were not collected for the subjects in this study, so these data were not available for comparison with the simulated muscle excitation timings.

A second limitation of musculoskeletal modeling is that some assumptions for musculoskeletal parameters are necessary.

However, the optimization algorithm can compensate for imprecise model parameters by adjusting the magnitude of the muscle excitations to produce the muscle forces necessary to track the experimental biomechanics. Therefore, it is likely that the muscle forces and resulting contributions to the subtasks of stair ascent were minimally affected by these modeling assumptions.

Another limitation is that the interface between the prosthesis and residual leg was not modeled in this study. However, the sockets were well-fitting and minimal pistoning was observed clinically. In addition, the orientation and loading of the limb during weight acceptance on stairs also likely minimizes the effect of pistoning. Therefore, losses at the interface were not expected to have impacted the overall conclusions regarding the nature of each muscle's contribution or the prosthesis's contribution to the biomechanical subtasks of stair ascent. However, for future work requiring precise magnitudes of these contributions, modeling this interface would be important.

One additional limitation is that group-averaged experimental data was simulated. Amputees have been shown to demonstrate different individual compensations which may not be apparent in the averaged data [14,48]. In an attempt to minimize inter-individual variability as much as possible prior to performing a group-average of the data, subjects ascended stairs at a fixed cadence. Based on a previous simulation study of healthy level walking, which found that relative muscle contributions were invariant with speed [33], we believe that controlling speed did not significantly affect the relative contributions identified in this study. However, as a result this simulation does not capture the variability of stair ascent gait identified across transtibial amputees. Similarly, the prosthesis was modeled using the average experimental amputee ankle moment data, for which the standard deviation was large due in part to varying ESAR prostheses worn by the subjects (Supplemental Table 1, which is available under the "Supplemental Data" tab for this paper on the ASME Digital Collection.) However, the direction of the moment remained consistent for up to nearly two standard deviations. Therefore, the nature of the prosthesis's contribution would be expected to remain the same, but the magnitude of the prosthesis's contribution may vary for an individual's specific prosthesis. For studies seeking to tune prostheses to individual needs or examining the effect of prosthesis type on resulting function, a more precise model of the prosthesis would be required. Future work should focus on generating subject-specific simulations of stair ascent at self-selected speed to enable the development of targeted rehabilitation programs tailored to an individual and their specific prosthesis. However, this study is an important first step toward understanding individual muscle and prosthesis contributions to the biomechanical subtasks of unilateral transtibial amputee stair ascent.

## 5 Summary

The passive ESAR prosthesis was found to provide vertical propulsion throughout stair ascent, similar to the role of the nonamputee plantarflexors. However the timing differed considerably and the contribution from gravity increased to compensate. The prosthesis also contributed to braking throughout stair ascent, similar to nonamputee SOL, but to a greater extent. However, the prosthesis was unable to replicate all of the functions of nonamputee GAS, which contributes to forward propulsion during the second half of stance and leg swing initiation. To compensate, residual HAM and VAS increased their contributions to forward propulsion during the first and second halves of stance, respectively, but overall the residual leg still contributed to braking. The prosthesis also contributed to medial control, consistent with the role of nonamputee SOL but not GAS.

## 6 Conclusions and Clinical Relevance

The results of this study provide insight into the compensations necessary for transtibial amputees to ascend stairs and have important implications for designing improved prostheses and restoring mobility in amputees. The results of this study indicate that amputee stair ascent could be improved and muscle compensations could be minimized through improved prosthesis designs that provide additional vertical propulsion, forward propulsion (or reduced braking), lateral control, and leg swing initiation at appropriate points in the gait cycle. For example, we demonstrate the prosthesis functions similarly to nonamputee SOL during early stance, slowing forward progression and likely contributing to the reliance on a hip-extensor strategy. These findings support the use of prostheses that allow or facilitate additional dorsiflexion motion during stair ascent [16] for individuals who are required to regularly ascend stairs during activities of daily living.

This study also provides important considerations for developing targeted rehabilitation programs to account for deficits in current prosthetic devices. For example, transtibial amputees can (1) increase their forward trunk lean during early residual leg stance, which will allow gravity to have a greater effect on forward propulsion, (2) increase force output by the intact plantarflexors during the second half of intact leg stance (first half of residual leg stance), which can contribute to vertical and forward propulsion, and (3) increase force output by residual HAM during the second half of residual leg stance to provide increased forward propulsion, lateral control, and leg swing initiation to compensate for the loss of GAS. These targeted rehabilitation strategies are critical because a prosthesis will likely be unable to replicate the functions of both nonamputee soleus and gastrocnemius, which contribute oppositely to several biomechanical subtasks of stair ascent.


## Acknowledgment

The authors would like to thank the members of the Military Performance Laboratory at the Center for the Intrepid for their contributions to subject recruitment and data collection and processing.

This study was supported in part by a National Science Foundation (NSF) Graduate Research Fellowship (DGE-1110007) and a research grant from the Center for Rehabilitation Sciences Research. The contents are solely the responsibility of the authors and do not necessarily represent the official views of the National Science Foundation. The views expressed herein are those of the authors and do not reflect the official policy or position of Brooke Army Medical Center, the U.S. Army Medical Department, the U.S. Army Office of the Surgeon General, the Department of the Army, Department of Defense or the U.S. Government.


## References


[1] Allen, J. L., and Neptune, R. R., 2012, "Three-Dimensional Modular Control of Human Walking," J. Biomech., **45**(12), pp. 2157–2163.

[2] Pandy, M. G., Lin, Y. C., and Kim, H. J., 2010, "Muscle Coordination of Mediolateral Balance in Normal Walking," J. Biomech., **43**(11), pp. 2055–2064.

[3] Neptune, R. R., Kautz, S. A., and Zajac, F. E., 2001, "Contributions of the Individual Ankle Plantar Flexors to Support, Forward Progression and Swing Initiation During Walking," J. Biomech., **34**(11), pp. 1387–1398.

[4] Liu, M. Q., Anderson, F. C., Pandy, M. G., and Delp, S. L., 2006, "Muscles That Support the Body Also Modulate Forward Progression During Walking," J. Biomech., **39**(14), pp. 2623–2630.

[5] Houdijk, H., Pollmann, E., Groenewold, M., Wiggerts, H., and Polomski, W., 2009, "The Energy Cost for the Step-to-Step Transition in Amputee Walking," Gait Posture, **30**(1), pp. 35–40.

[6] Genin, J. J., Bastien, G. J., Franck, B., Detrembleur, C., and Willems, P. A., 2008, "Effect of Speed on the Energy Cost of Walking in Unilateral Traumatic Lower Limb Amputees," Eur. J. Appl. Physiol., **103**(6), pp. 655–663.

[7] Prinsen, E. C., Nederhand, M. J., and Rietman, J. S., 2011, "Adaptation Strategies of the Lower Extremities of Patients With a Transtibial or Transfemoral Amputation During Level Walking: A Systematic Review," Arch. Phys. Med. Rehabil., **92**(8), pp. 1311–1325.

[8] Silverman, A. K., and Neptune, R. R., 2011, "Differences in Whole-Body Angular Momentum Between Below-Knee Amputees and Non-Amputees Across Walking Speeds," J. Biomech., **44**(3), pp. 379–385.

[9] Sheehan, R. C., Beltran, E. J., Dingwell, J. B., and Wilken, J. M., 2015, "Mediolateral Angular Momentum Changes in Persons With Amputation During Perturbed Walking," Gait Posture, **41**(3), pp. 795–800.

[10] Nadeau, S., McFadyen, B. J., and Malouin, F., 2003, "Frontal and Sagittal Plane Analyses of the Stair Climbing Task in Healthy Adults Aged Over 40 Years: What Are the Challenges Compared to Level Walking?," Clin. Biomech., **18**(10), pp. 950–959.
[11] DeVita, P., Helseth, J., and Hortobagyi, T., 2007, "Muscles Do More Positive Than Negative Work in Human Locomotion," J. Exp. Biol., **210**(Pt 19), pp. 3361–3373.
[12] Novak, A. C., and Brouwer, B., 2011, "Sagittal and Frontal Lower Limb Joint Moments During Stair Ascent and Descent in Young and Older Adults," Gait Posture, **33**(1), pp. 54–60.
[13] Wilken, J. M., Sinitski, E. H., and Bagg, E. A., 2011, "The Role of Lower Extremity Joint Powers in Successful Stair Ambulation," Gait Posture, **34**(1), pp. 142–144.
[14] Powers, C. M., Boyd, L. A., Torburn, L., and Perry, J., 1997, "Stair Ambulation in Persons With Transtibial Amputation: An Analysis of the Seattle LightFoot," J. Rehabil. Res. Dev., **34**(1), pp. 9–18.
[15] Schmalz, T., Blumentritt, S., and Marx, B., 2007, "Biomechanical Analysis of Stair Ambulation in Lower Limb Amputees," Gait Posture, **25**(2), pp. 267–278.
[16] Alimusaj, M., Fradet, L., Braatz, F., Gerner, H. J., and Wolf, S. I., 2009, "Kinematics and Kinetics With an Adaptive Ankle Foot System During Stair Ambulation of Transtibial Amputees," Gait Posture, **30**(3), pp. 356–363.
[17] Yack, J. H., Nielsen, D. H., and Shurr, D. G., 1999, "Kinetic Patterns During Stair Ascent in Patients With Transtibial Amputations Using Three Different Prostheses," J. Prosthetics Orthotics, **11**(3), pp. 57–62.
[18] Sinitski, E. H., Hansen, A. H., and Wilken, J. M., 2012, "Biomechanics of the Ankle-Foot System During Stair Ambulation: Implications for Design of Advanced Ankle-Foot Prostheses," J. Biomech., **45**(3), pp. 588–594.
[19] Agrawal, V., Gailey, R. S., Gaunaurd, I. A., O'Toole, C., and Finnieston, A. A., 2013, "Comparison Between Microprocessor-Controlled Ankle/Foot and Conventional Prosthetic Feet During Stair Negotiation in People With Unilateral Transtibial Amputation," J. Rehabil. Res. Dev., **50**(7), pp. 941–950.
[20] Torburn, L., Schweiger, G. P., Perry, J., and Powers, C. M., 1994, "Below-Knee Amputee Gait in Stair Ambulation. A Comparison of Stride Characteristics Using Five Different Prosthetic Feet," Clin. Orthop. Relat. Res., **303**, pp. 185–192.
[21] Aldridge, J. M., Sturdy, J. T., and Wilken, J. M., 2012, "Stair Ascent Kinematics and Kinetics With a Powered Lower Leg System Following Transtibial Amputation," Gait Posture, **36**(2), pp. 291–295.
[22] Zmitrewicz, R. J., Neptune, R. R., and Sasaki, K., 2007, "Mechanical Energetic Contributions From Individual Muscles and Elastic Prosthetic Feet During Symmetric Unilateral Transtibial Amputee Walking: A Theoretical Study," J. Biomech., **40**(8), pp. 1824–1831.
[23] Silverman, A. K., and Neptune, R. R., 2012, "Muscle and Prosthesis Contributions to Amputee Walking Mechanics: A Modeling Study," J. Biomech., **45**(13), pp. 2271–2278.
[24] Harper, N. G., Wilken, J. M., and Neptune, R. R., 2018, "Muscle Function and Coordination of Stair Ascent," ASME J. Biomech. Eng., **140**(1), p. 011001.
[25] Lin, Y. C., Fok, L. A., Schache, A. G., and Pandy, M. G., 2015, "Muscle Coordination of Support, Progression and Balance During Stair Ambulation," J. Biomech., **48**(2), pp. 340–347.
[26] Delp, S. L., Loan, J. P., Hoy, M. G., Zajac, F. E., Topp, E. L., and Rosen, J. M., 1990, "An Interactive Graphics-Based Model of the Lower Extremity to Study Orthopaedic Surgical Procedures," IEEE Trans. Biomed. Eng., **37**(8), pp. 757–767.
[27] Davy, D. T., and Audu, M. L., 1987, "A Dynamic Optimization Technique for Predicting Muscle Forces in the Swing Phase of Gait," J. Biomech., **20**(2), pp. 187–201.
[28] Neptune, R. R., Wright, I. C., and Van Den Bogert, A. J., 2000, "A Method for Numerical Simulation of Single Limb Ground Contact Events: Application to Heel-Toe Running," Comput. Methods Biomech. Biomed. Eng., **3**(4), pp. 321–334.
[29] Raasch, C. C., Zajac, F. E., Ma, B., and Levine, W. S., 1997, "Muscle Coordination of Maximum-Speed Pedaling," J. Biomech., **30**(6), pp. 595–602.
[30] Winters, J. M., and Stark, L., 1988, "Estimated Mechanical Properties of Synergistic Muscles Involved in Movements of a Variety of Human Joints," J. Biomech., **21**(12), pp. 1027–1041.
[31] Zajac, F. E., 1989, "Muscle and Tendon: Properties, Models, Scaling, and Application to Biomechanics and Motor Control," Crit. Rev. Biomed. Eng., **17**(4), pp. 359–411.
[32] Goffe, W. L., Ferrier, G. D., and Rogers, J., 1994, "Global Optimization of Statistical Functions With Simulated Annealing," J. Econometrics, **60**(1–2), pp. 65–99.
[33] Neptune, R. R., Sasaki, K., and Kautz, S. A., 2008, "The Effect of Walking Speed on Muscle Function and Mechanical Energetics," Gait Posture, **28**(1), pp. 135–143.
[34] Neptune, R. R., Zajac, F. E., and Kautz, S. A., 2004, "Muscle Force Redistributes Segmental Power for Body Progression During Walking," Gait Posture, **19**(2), pp. 194–205.
[35] Lin, Y. C., Kim, H. J., and Pandy, M. G., 2011, "A Computationally Efficient Method for Assessing Muscle Function During Human Locomotion," Int. J. Numer. Methods Biomed. Eng., **27**(3), pp. 436–449.
[36] Anderson, F. C., and Pandy, M. G., 2003, "Individual Muscle Contributions to Support in Normal Walking," Gait Posture, **17**(2), pp. 159–169.
[37] Della Croce, U., and Bonato, P., 2007, "A Novel Design for an Instrumented Stairway," J. Biomech., **40**(3), pp. 702–704.
[38] Wilken, J. M., Rodriguez, K. M., Brawner, M., and Darter, B. J., 2012, "Reliability and Minimal Detectible Change Values for Gait Kinematics and Kinetics in Healthy Adults," Gait Posture, **35**(2), pp. 301–307.
[39] Dempster, W. T., 1955, "Space Requirements of the Seated Operator: Geometrical, Kinematic, and Mechanical Aspects of the Body With Special Reference to the Limbs," *Wright Air Development Center Technical Report*, Wright-Patterson Air Force Base, Dayton, OH.
[40] Grood, E. S., and Suntay, W. J., 1983, "A Joint Coordinate System for the Clinical Description of Three-Dimensional Motions: Application to the Knee," ASME J. Biomech. Eng., **105**(2), pp. 136–144.
[41] Wu, G., and Cavanagh, P. R., 1995, "ISB Recommendations for Standardization in the Reporting of Kinematic Data," J. Biomech., **28**(10), pp. 1257–1261.
[42] Wu, G., Siegler, S., Allard, P., Kirtley, C., Leardini, A., Rosenbaum, D., Whittle, M., D'Lima, D. D., Cristofolini, L., Witte, H., Schmid, O., and Stokes, I., 2002, "ISB Recommendation on Definitions of Joint Coordinate System of Various Joints for the Reporting of Human Joint Motion—Part I: Ankle, Hip, and Spine," J. Biomech., **35**(4), pp. 543–548.
[43] Baker, R., 2001, "Pelvic Angles: A Mathematically Rigorous Definition Which Is Consistent With a Conventional Clinical Understanding of the Terms," Gait Posture, **13**(1), pp. 1–6.
[44] Ramstrand, N., and Nilsson, K. A., 2009, "A Comparison of Foot Placement Strategies of Transtibial Amputees and Able-Bodied Subjects During Stair Ambulation," Prosthetics Orthotics Int., **33**(4), pp. 348–355.
[45] Kendell, C., Lemaire, E. D., Dudek, N. L., and Kofman, J., 2010, "Indicators of Dynamic Stability in Transtibial Prosthesis Users," Gait Posture, **31**(3), pp. 375–379.
[46] Zajac, F. E., and Gordon, M. E., 1989, "Determining Muscle's Force and Action in Multi-Articular Movement," Exercise Sport Sci. Rev., **17**(1), pp. 187–230.
[47] Zajac, F. E., Neptune, R. R., and Kautz, S. A., 2002, "Biomechanics and Muscle Coordination of Human Walking. Part I: Introduction to Concepts, Power Transfer, Dynamics and Simulations," Gait Posture, **16**(3), pp. 215–232.
[48] Silverman, A. K., Fey, N. P., Portillo, A., Walden, J. G., Bosker, G., and Neptune, R. R., 2008, "Compensatory Mechanisms in Below-Knee Amputee Gait in Response to Increasing Steady-State Walking Speeds," Gait Posture, **28**(4), pp. 602–609.